



Seismic stability evaluation using 2-D FEM analysis for modeling nuclear power plants sited on gravel soil

Iba, T.¹, Konno, T.², Irino, K.³, Hama, I.⁴, Oguro, E.⁵, Iizuka, S.⁶, Enami, A.⁷

1) Obayashi Corporation, Tokyo, Japan

2) Kajima Corporation, Tokyo, Japan

3) Shimizu Corporation, Tokyo, Japan

4) Taisei Corporation, Tokyo, Japan

5) Takenaka Corporation, Tokyo, Japan

6) Nuclear Power Engineering Corporation, Tokyo, Japan

7) Nihon University, Tokyo, Japan

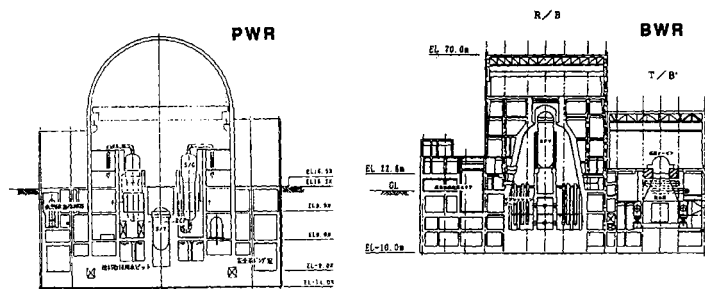
1. INTRODUCTION

Throughout Europe and the United States, many nuclear power plants have been built on Quaternary deposit sites. While in Japan, all nuclear power plants have been built at rock sites primarily to maintain a high seismic resistivity. However, as more nuclear power plants are planned for the future, it has become necessary to develop new siting technology from the stand point of expanding the available range of site selection and effective utilization of land. A draft on guidelines of the seismic design for siting on Quaternary deposits is being carried out with a purpose to ensure proper design and construction for such sites.

2. PURPOSE

Ensuring seismic stability of the foundation soil is one of the most important issues for constructing a nuclear power plant on Quaternary deposits. Therefore, a seismic stability analysis using a 2-D FEM has been performed, and an evaluation of the analysis is presented in this study. The study nuclear power plants are a BWR and PWR (Figure 1).

Figure 1. The study nuclear power plants



3. STUDY SCHEME

The study scheme consisted of three main topics; a stress analysis under normal conditions, a seismic response analysis, and an evaluation of the foundation soil stability. A flow chart of the study is shown in Figure 2. For normal conditions, a non-linear static analysis using the Duncan-Chang model is performed, stress and settlement of the soil layers are calculated, and the corresponding soil deformation characteristics obtained. With these known soil characteristics, a dynamic equivalent linearization seismic response analysis is carried out using the Hardin-Drnevich model, and the stresses and strains of the soil layers are calculated. Finally, by summing the static and dynamic stresses and strains induced by the earthquake with those of the normal condition, the seismic stability is evaluated. All analyses were performed using a 2-dimensional soil-structure interaction model.

4. ANALYSIS MODEL

The structural portion of the analysis model is multi-lumped mass with shear-bending beam elements. The soil portion of the analysis model consists of plane strain elements. Shear wave velocities assumed at the top of the bearing soil layer are 400m/s for the PWR (Vs400) and 350m/s for the BWR (Vs350) because, from a previous study, a Vs300 model did not provide

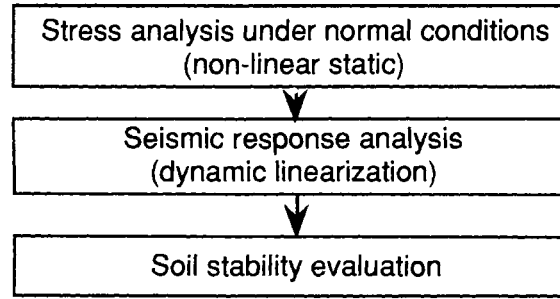


Figure 2. Study flow chart

seismic stability. The Vs400 and Vs350 models are shown in Figure 3. Soil properties were determined from tests conducted on high quality undisturbed samples, namely frozen samples, of Quaternary sand and gravel deposits from the Tadotsu site. The soil properties determined are shown in Table 1.

In order to avoid liquefaction of the surface soil, the ground water level is defined at the top of the bearing soil layer of the structure, which corresponds to structure elevations of EL= -14 m and EL= -10 m for the PWR and BWR respectively.

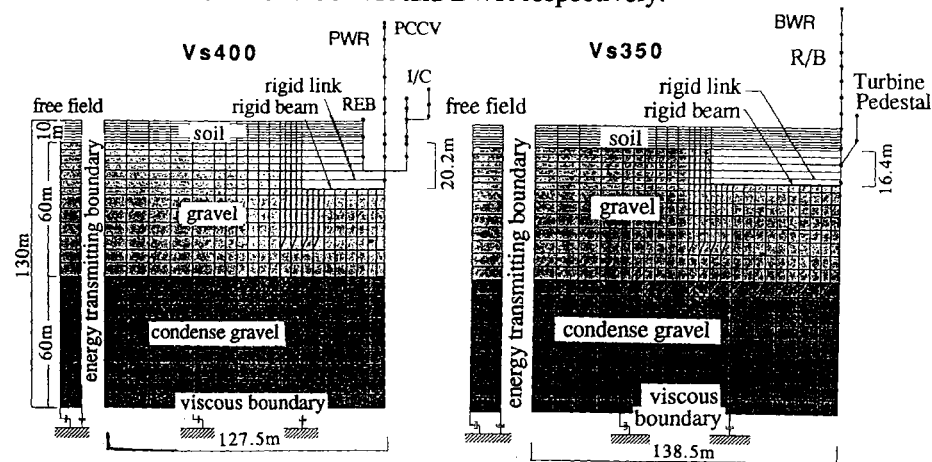


Figure 3. Analysis Models

Earthquake motion used in the analysis is determined on the basis of observed earthquake motions obtained at Quaternary deposits, and it is shown in Figure 4. Assuming this earthquake motion to be defined at the level of GL=-10m, earthquake input motion for the bottom of the 2-dimensional analysis model (GL=-130m) is determined using the SHAKE analysis code.

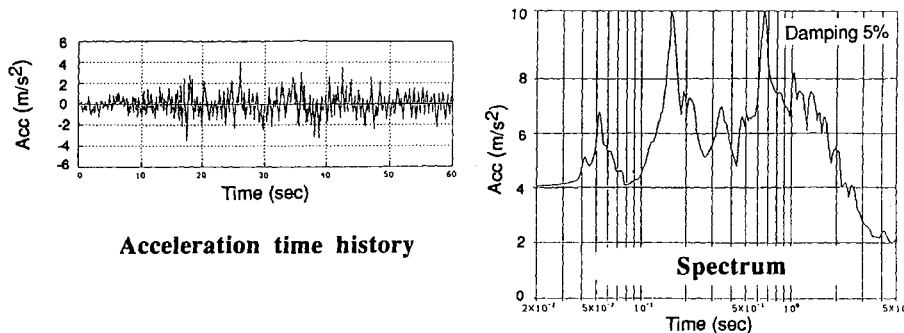


Figure 4. Earthquake input motion

Table 1. Soil Characteristics

PWR with Vs=400m/sec													BWR with Vs=350m/sec												
#	EP t/m ²	σ _{m'} t/m ²	γ t/m ³	φ °	C t/m ²	V _s m/sec	G ₀ t/m ²	τ _r t/m ²	γ _r ×10 ⁻³	ν	h _{max} %	#	EP t/m ²	σ _{m'} t/m ²	γ t/m ³	φ °	C t/m ²	V _s m/sec	G ₀ t/m ²	τ _r t/m ²	γ _r ×10 ⁻³	ν	h _{max} %		
1	0.00 ~ 1.58	0.79	1.9	36.0	0.0	140	3800	0.52	0.138	0.33	20	1	0.00 ~ 1.58	0.79	1.9	36.0	0.0	140	3800	0.52	0.138	0.33	20		
2	1.58 ~ 3.16	2.37				190	7000	1.57	0.224			2	1.58 ~ 3.16	2.37				190	7000	1.57	0.224				
3	3.16 ~ 4.74	3.95				210	8600	2.62	0.304			3	3.16 ~ 4.74	3.95				210	8600	2.62	0.304				
4	4.74 ~ 6.32	5.53				230	10000	3.66	0.366			4	4.74 ~ 6.32	5.53				230	10000	3.66	0.366				
5	6.32 ~ 7.90	7.11				250	12000	4.71	0.393			5	6.32 ~ 7.90	7.11				250	12000	4.71	0.393				
6	7.90 ~ 9.48	8.69				260	13000	5.76	0.443			6	7.90 ~ 9.48	8.69				260	13000	5.76	0.443				
7	9.48 ~ 11.1	10.3				270	14000	6.81	0.486			7	9.48 ~ 11.1	10.3				270	14000	6.81	0.486				
8	11.1 ~ 12.6	11.9				280	15000	7.85	0.523			8	11.1 ~ 12.6	11.9				280	15000	7.85	0.523				
9	15.0 ~ 25.0	20.0	2.3	40.0	5.0	420	41000	17.00	0.414		13	9	15.0 ~ 25.0	20.0	2.3	38.0	2.0	370	32000	14.30	0.447		15		
10	25.0 ~ 35.0*	30.0				460	50000	22.70	0.455	0.33		10	25.0 ~ 35.0*	30.0				410	39000	20.40	0.523	0.33			
										0.49												0.40			
										0.33												0.49			
11	35.0 ~ 45.0*	40.0				500	59000	29.90	0.507	0.40		11	35.0 ~ 45.0*	40.0				440	45000	27.50	0.612	0.40			
										0.49												0.40			
12	45.0 ~ 55.0*	50.0				530	66000	38.20	0.579	0.40		12	45.0 ~ 55.0*	50.0				460	50000	34.00	0.680	0.40			
										0.49												0.40			
13	55.0 ~ 65.0	60.0				550	71000	44.50	0.627	0.49		13	55.0 ~ 65.0	60.0				480	55000	40.70	0.754	0.49			
14	65.0 ~ 75.0	70.0				570	76000	51.40	0.677			14	65.0 ~ 75.0	70.0				500	59000	46.70	0.792				
15	75.0 ~ 85.0	80.0				590	82000	57.80	0.705			15	75.0 ~ 85.0	80.0				520	63000	53.30	0.846				
16	85.0 ~ 95.0	90.0				600	84000	64.60	0.769			16	85.0 ~ 95.0	90.0				530	66000	60.40	0.915				
17	95.0 ~ 105.0	100.0						71.40	0.850			17	95.0 ~ 105.0	100.0		40.0				68.30	1.030				
18	105.0 ~ 115.0	110.0						77.30	0.921			18	105.0 ~ 115.0	110.0						75.50	1.140				
19	115.0 ~ 125.0	120.0						84.30	1.000			19	115.0 ~ 125.0	120.0						82.50	1.250				
20	125.0 ~ 135.0	130.0						91.50	1.090			20	125.0 ~ 135.0	130.0						88.70	1.340				
21	135.0 ~ 145.0	140.0						97.50	1.160			21	135.0 ~ 145.0	140.0						95.70	1.450				
22	145.0 ~ 155.0	150.0						104.00	1.240			22	145.0 ~ 155.0	150.0						103.00	1.550				
23	155.0 ~ 165.0	160.0						111.00	1.320			23	155.0 ~ 165.0	160.0						108.00	1.630				

#: Layer number
 EP: Effective confined pressure
 $\sigma_{m'} = (\sigma_1 + \sigma_2' + \sigma_3')/3$
 φ: Friction angle
 C: Cohesion
 Vs: Shear wave velocity
 $G_0 = \gamma/g \cdot V_s^2$
 $\tau_r = C \cos \phi + (\sigma_1' + \sigma_3')/2 \cdot \sin \phi$
 $\gamma_r = \tau_r / G_0$
 ν: Poisson's ratio
 h_{max}: Maximum damping
 * Above ground water level, Poisson's ratio is 0.40 but 0.33 for shallow regions, and below ground water level the ratio is 0.49

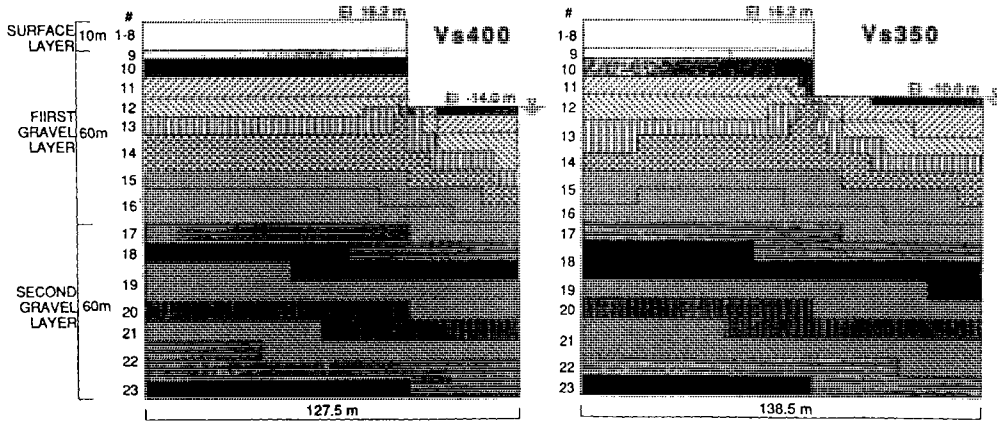


Figure 5. Soil model pattern layout for dynamic linearization analysis

5. ANALYSIS RESULTS

5.1 Structure Response

Maximum responses for the PWR and BWR structures are shown in the Table 2.

Table 2. Maximum responses of the structures

	Acceleration (m/s ²)		Relative Displacement (m)		Max shear stress (KPa)
	bottom of basemat	top of structure	bottom of basemat	top of structure	
PWR	4.02	6.43	0.0039	0.0137	1550
BWR	4.45	5.42	0.0051	0.0168	2226

5.2 Soil Response

In Figure 6 the maximum soil shear strains for the Vs400 and Vs350 models are shown. The soil maximum shear strain generally ranges from $0.5-2.5 \times 10^{-3}$. In addition to the shear strains, Figure 6 displays the maximum accelerations for the soil at the center line of the reactor buildings. The soil maximum accelerations are 4.02 and 4.45 m/s^2 for the Vs400 and Vs350 models respectively.

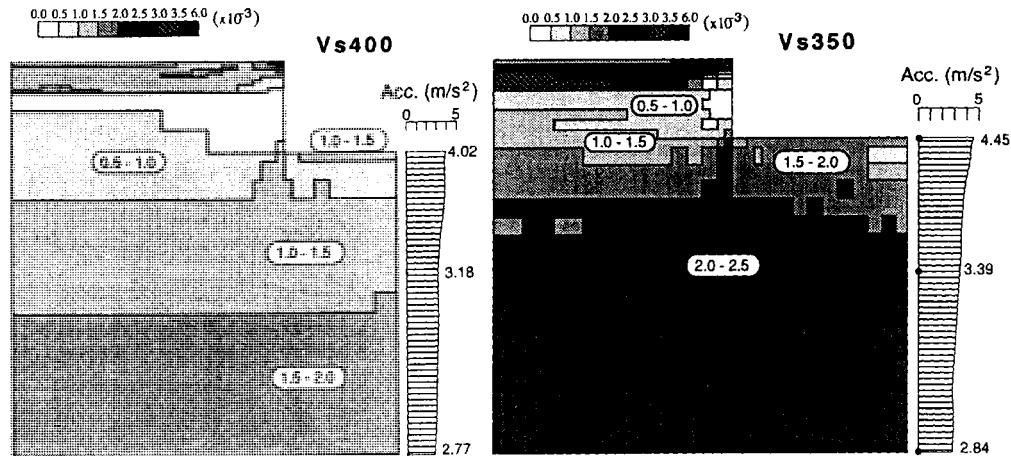


Figure 6. Maximum shear strain and acceleration of the soil

6. SOIL STABILITY EVALUATION

6.1 Dynamic Strength of the Foundation Soil (Cyclic Mobility)

Dynamic shear strength of the foundation soil subjected to seismic motion is investigated. The investigation focuses on a point below the ground water level, and where the pore water pressure increases, it is examined whether cyclic mobility is present. Using the maximum value of dynamic shear stress in a time domain, the safety factor of dynamic failure is determined from the following equations.

Safety Factor, $F_1 = R/L$

$$L = \tau_{eq} / \sigma_{mo}'$$

$$\sigma_{mo}' = \frac{1}{3} (\sigma_{xo}' + \sigma_{yo}' + \sigma_{zo}')$$

where

R : dynamic strength (shear stress / confining stress)

τ_{eq} : $0.65\tau_{max}$

τ_{max} : maximum dynamic shear stress

σ_{xo}' , σ_{yo}' , σ_{zo}' : initial effective normal stresses corresponding to three cartesian coordinates

Figure 7 displays the L values for the bearing soil at the center line of the PWR and BWR reactor buildings. For fixing the R value, a test is currently being conducted, and the value is expected to be greater than L .

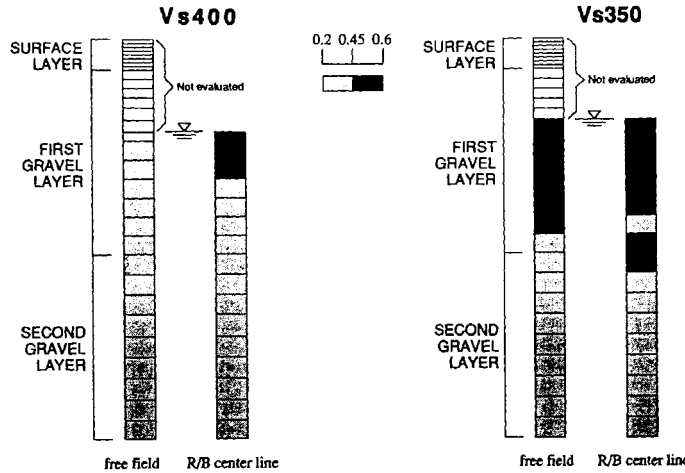


Figure 7. L value (effective shear stress / confining stress)

6.2 Local Stability of the Foundation Soil

In order to determine a local stability of the foundation soil, the time history of local safety coefficients is worked out, and the minimum coefficient is picked out. The local safety coefficient is the combination of normal operating and seismic stress conditions, and it can be calculated from the method shown in Figure 8.

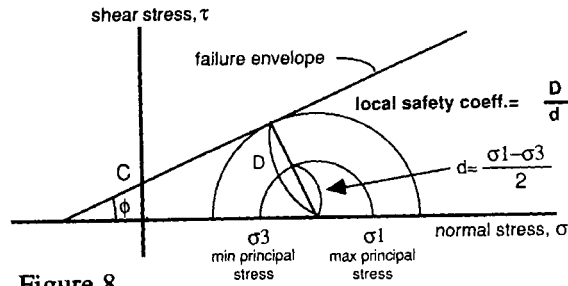


Figure 8.

For the Vs400 model, the local safety factor coefficients are generally around 1.0, with the exception of the area in the vicinity of the basemat edges where the coefficients vary between 0.8 and 1.0. For the Vs350 model, the safety factor coefficients vary from 0.8 to 1.2 in areas just below the basemat, and from 0.2 to 0.4 in the vicinity of the structure's side and basemat edges. Distribution of the local safety factors are shown in Figure 9.

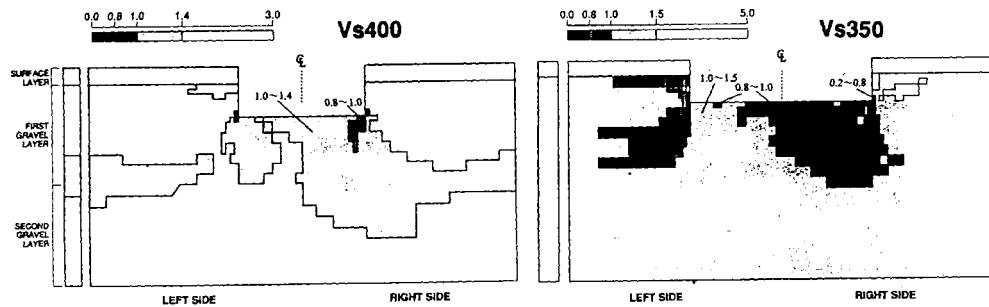


Figure 9. Safety factor for local stability

6.3 Slip Stability of Foundation Soil

In order to determine a slip stability of the foundation soil, the time history is worked out to find safety factors along an assumed slip surface. Appropriately, the minimum slip safety factors are picked out from the search, and they are used for the soil slip stability study. Safety factors for the normal and dynamic conditions are combined together, and they are calculated from the following equation.

$$\text{slip surface safety factor} = \frac{\sum \tau_{fi} \cdot l_i}{\sum \tau_{si} \cdot l_i}$$

where

τ_{fi} : *i*th component of the shear strength τ_f

τ_{si} : *i*th component of shear stress τ_s along the potential slip plane

l_i : *i*th component slip plane length

Figure 10 shows the model for the slip failure for which the above equation is applied. The slip safety factor is analyzed for left and right side standard slip plane angle combinations of 20, 30, 40, 50, and 60 degrees. The minimum safety factor for Vs400 is 1.85 occurring at a slip angle combination of 20° (right side) and 60° (left side). For the Vs350 case, the factor is 1.28 with the same slip angle combination.

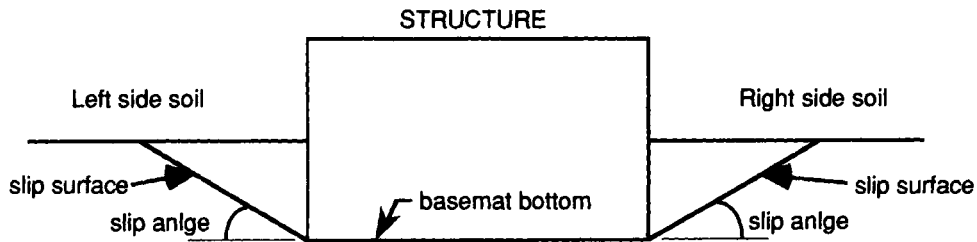


Figure 10. Model for slip failure

7. CONCLUSION

1. The response analysis of nuclear power plants to be sited on Quaternary deposits should consider non-linearity in the soil-structure interaction.
2. From the analysis results, three features of the foundation soil were estimated as follows:
 - a. Dynamic strength of the foundation soil
 - b. Local stability of the foundation soil
 - c. Slip stability of the foundation soil
3. From the above features, it was confirmed that nuclear power plant construction on Quaternary deposit, for both analysis cases (Vs=400, 350 m/s), is feasible.

8. ACKNOWLEDGMENT

This work was carried out by Nuclear Power Engineering Corporation (NUPEC) as the entrusted project sponsored by the Ministry of International Trade and Industry in Japan. This work was supported by "Committee on Verification Test of Quaternary Siting Technology" of NUPEC. The authors wish to express their gratitude for the cooperation and valuable suggestions given by the members of the Committee.